

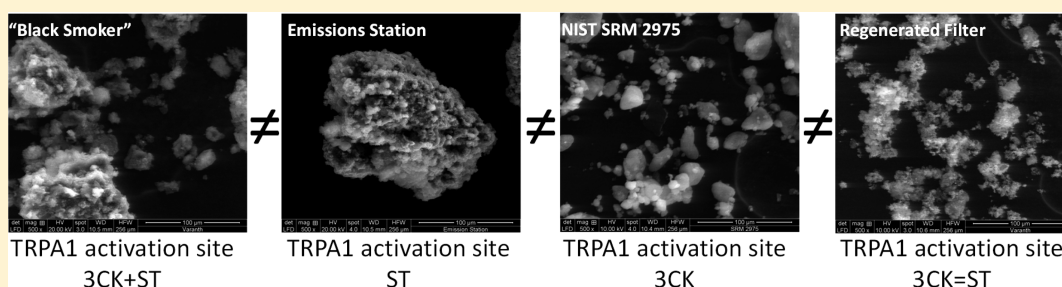
# Differential Activation of TRPA1 by Diesel Exhaust Particles: Relationships between Chemical Composition, Potency, and Lung Toxicity

Cassandra E. Deering-Rice,<sup>†</sup> Tosifa Memon,<sup>†</sup> Zhenyu Lu,<sup>†</sup> Erin G. Romero,<sup>†</sup> James Cox,<sup>‡</sup> Thomas Taylor-Clark,<sup>§</sup> John M. Veranth,<sup>†</sup> and Christopher A. Reilly<sup>\*,†</sup>

<sup>†</sup>Department of Pharmacology & Toxicology, Center for Human Toxicology and <sup>‡</sup>Department of Biochemistry, University of Utah, 30 South 2000 East, Salt Lake City, Utah 84112, United States

<sup>§</sup>Department of Molecular Pharmacology & Physiology, Morsani College of Medicine, University of South Florida, Tampa, Florida 33612, United States

## Supporting Information



**ABSTRACT:** Diesel exhaust particulate (DEP) causes pulmonary irritation and inflammation, which can exacerbate asthma and other diseases. These effects may arise from the activation of transient receptor potential ankyrin-1 (TRPA1). This study shows that a representative DEP can activate TRPA1-expressing pulmonary C-fibers in the mouse lung. Furthermore, DEP collected from idling vehicles at an emissions inspection station, the tailpipe of an on-road “black smoker” diesel truck, waste DEP from a diesel exhaust filter regeneration machine, and NIST SRM 2975 can activate human TRPA1 in lung epithelial cells to elicit different biological responses. The potency of the DEP, particle extracts, and selected chemical components was compared in TRPA1 over-expressing HEK-293 and human lung cells using calcium flux and other toxicologically relevant endpoint assays. Emission station DEP was the most potent and filter DEP the least. Potency was related to the percentage of ethanol extractable TRPA1 agonists and was equivalent when equal amounts of extract mass was used for treatment. The DEP samples were further compared using scanning electron microscopy, energy-dispersive X-ray spectroscopy, gas chromatography–mass spectrometry, and principal component analysis as well as targeted analysis of known TRPA1 agonists. Activation of TRPA1 was attributable to both particle-associated electrophiles and non-electrophilic agonists, which affected the induction of interleukin-8 mRNA via TRPA1 in A549 and IMR-90 lung cells as well as TRPA1-mediated mucin gene induction in human lung cells and mucous cell metaplasia in mice. This work illustrates that not all DEP samples are equivalent, and studies aimed at assessing mechanisms of DEP toxicity should account for multiple variables, including the expression of receptor targets such as TRPA1 and particle chemistry.

## INTRODUCTION

Particulate air pollution is associated with acute and chronic adverse health effects in humans. However, the biochemical mechanisms linking particle inhalation to specific cellular and systemic biological effects are not fully understood. A frequent constituent of environmental particulate matter (PM) in urban areas is diesel exhaust particles (DEP).<sup>1</sup> DEP has been studied extensively and has been reported to cause adverse respiratory and cardiovascular outcomes including acute lung inflammation, airway irritation, cardiac arrhythmias, and possibly cancer.<sup>2,3</sup>

An emerging hypothesis explaining how different constituents of heterogeneous environmental PM causes adverse

effects centers on the activation of transient receptor potential (TRP) ion channels. TRP Ankyrin-1 (TRPA1), Vanilloid-1–4 (TRPV1–4), Melastatin-2 and –8 (TRPM2 and M8), and other TRPs, are variably expressed in the respiratory tract, where they function as environmental sensors, responding to variations in temperature and the presence of specific chemical entities including endogenous inflammatory mediators and exogenous irritants.<sup>4–6</sup> Activation of TRPA1 has been linked to cardiovascular changes associated with pulmonary DEP exposure in rats,<sup>3</sup> development of asthma-like phenotypes in

Received: November 30, 2018

Published: April 4, 2019

mice,<sup>7</sup> and suboptimal asthma control in patients expressing gain-of-function polymorphic variants in both TRPA1 and TRPV1.<sup>8,9</sup> In several studies, it has been shown that TRPA1 mediates acute respiratory responses to electrophilic and oxidizing environmental pollutants including acrolein and crotonaldehyde,<sup>10,11</sup> as well as to H<sub>2</sub>O<sub>2</sub> and HOCl.<sup>12</sup> TRPA1 can also be activated by DEP via the release of particle-associated electrophiles and non-electrophilic chemicals and through mechanical perturbation by insoluble components.<sup>8,13</sup> Mechanistically, activation of TRPA1 in pulmonary C-fibers promotes neurogenic inflammation.<sup>14</sup> Additionally, TRPA1 is expressed by some epithelial-type cells of the airways and alveoli, where activation can alter pro-inflammatory cytokine/chemokine expression among other toxicologically relevant responses.<sup>15,16</sup>

There is abundant literature describing properties of DEP that affect its potency and toxicity. However, due to the wide variability and complexity of these materials in the environment and in experimental platforms, well-defined mechanisms are lacking, and often, previously described mechanisms fail to fully explain the effects of different forms of DEP in different test systems. In the present study, we investigated questions specific to the role of TRPA1 as a mediator of DEP toxicity in the lung. The questions were: (1) Are TRPA1-expressing pulmonary C-fibers activated by DEP in an intact, uninjured lung? (2) Is TRPA1 uniquely activated by different types of DEP? (3) Does the biochemical mechanism of TRPA1 activation vary as a function of the chemical composition of the DEP? (4) Do variations in TRPA1 activation by DEP translate into differences in commonly observed cellular responses to DEP (e.g., cytokine gene induction) in lung cell lines that express TRPA1? and (5) Do variations in TRPA1 activation by DEP promote differences lung inflammation and injury in mice?

## MATERIALS AND METHODS

**Chemicals and DEP.** Allyl-isothiocyanate (AITC), perinaphthene, (3E)-[1-phenyl-1,3-pentadieny]benzene (3EPPB), 2,4- and 3,5-ditert butylphenol, EPA 8310 polynuclear aromatic hydrocarbon mix (certified reference material), aldehyde and ketone TO11/IP-6A aldehyde/ketone-DNPH mix, and all other chemicals were purchased from Sigma-Aldrich (St. Louis, MO) unless otherwise specified. A967079 was purchased from Cayman Chemical (Ann Arbor, MI). Information regarding the “black smoker” DEP source and composition can be found in prior publications by our group.<sup>13,17</sup> NIST SRM 2975 DEP was purchased. The emissions station DEP was collected from idling diesel-powered vehicles during emissions testing. The regenerated diesel particle filter sample is waste material after filter regeneration and was collected from a local mechanic’s shop. The mean hydrodynamic radii of the DEP, as determined using dynamic light scattering (DLS; Möbius, Wyatt Technology Corporation), were: black smoker, 116 ± 6; regenerated filter, 105 ± 5; NIST SRM 2975, 85.7 ± 0.6; and emissions station, 470 ± 50. Measurement of the emissions station DEP was challenging due to instability of the suspension and a rapid settling rate. DLS measurements were performed on samples suspended in DI water (30 µg/mL) at 25 °C with a detection angle of 163.5°. Cell culture treatments using DEP were prepared by suspending the particles in LHC-9 cell culture media at 3× final treatment concentration. DEP extracts were prepared by shaking the DEP in ethanol overnight at room temperature, followed by centrifugation and filtration through a 0.22 µm syringe filter. The filtrate was dried, weighed and suspended in DMSO prior to dilution in LHC-9 (2% DMSO) for cell treatments, as previously described.<sup>13</sup> Extract potency was compared in two ways: (1) based on an equivalent original DEP mass and (2) based on an equivalent extract residue mass.

**Animals.** Experimental protocols were approved by either the University of Utah or University of South Florida Animal Care and Use (IACUC) committees. Mice were maintained under normal housing conditions without restrictions.

**C-Fiber Extracellular Recordings.** The innervated isolated trachea/bronchus preparation was prepared as previously described.<sup>18</sup> Briefly, 6–10 week old male C57BL/6 mice were used. Mice were sacrificed using CO<sub>2</sub> followed by exsanguination. Next, the airways and lungs with their intact extrinsic innervation (vagus nerve including vagal ganglia) were dissected in Krebs bicarbonate buffer solution composed of (in millimolar) 118, NaCl; 5.4, KCl; 1.0, NaH<sub>2</sub>PO<sub>4</sub>; 1.2, MgSO<sub>4</sub>; 1.9, CaCl<sub>2</sub>; 25.0, NaHCO<sub>3</sub>; and 11.1, dextrose and equilibrated with 95% O<sub>2</sub> and 5% CO<sub>2</sub> (pH 7.2–7.4) (also containing indomethacin (3 mM)). The airways were pinned down and a vagal ganglion was gently pulled into an adjacent compartment of the assay chamber through a small hole and pinned. Both compartments were separately perfused with buffer (37 °C). A sharp glass electrode (3 M NaCl solution) was inserted into the vagal ganglion to record action potentials that were amplified (Micro-electrode AC amplifier 1800; A-M Systems, Everett, WA) and filtered (0.3 kHz of low cutoff and 1 kHz of high cutoff). Data were captured and analyzed using NerveOfIt software (Phocis, Baltimore, MD). The conduction velocity was calculated by dividing the distance along the nerve pathway by the time delay between the shock artifact and the action potential evoked by electrical stimulation of the airways. Only fibers with conduction velocities <0.7 m/s (C-fibers) were studied. Drugs and DEP were intratracheally applied as a 1 mL bolus over 10 s.

Individual sensory nerve responses were only studied following a positive response to stimulation of the lungs with both electrical and mechanical (von Frey fiber) stimuli. AITC (300 µM) was applied to identify TRPA1-expressing fibers, followed by a 15 min wash-out. The lungs were then treated with DEP (1 mg/mL, infused). At the end of the experiment, the lungs were treated with capsaicin (1 µM), which activates airway sensory nerves with conduction velocities of <0.75 m/s via TRPV1.

**Physical and Chemical Analysis of DEP.** Scanning electron microscopy (SEM) and energy dispersive X-ray spectroscopy (EDS) were performed on an FEI Quanta 600 FEG microscope system through the University of Utah NANOFAB Institute core services. The dry DEP powders, as obtained, were gently sprinkled onto imaging disks, and assayed. High-resolution gas chromatography mass spectrometry (GC-MS), principal component analysis (PCA) of spectral data, and selected target analyte assays of DEP samples were performed by the University of Utah Metabolomics Core facility. Analysis of the DEP materials by liquid chromatography–tandem mass spectrometry (LC-MS/MS) was performed as previously described.<sup>19</sup>

**Cells.** Cells were maintained in a humidified cell culture incubator at 37 °C with a 95% air/5% CO<sub>2</sub>. HEK-293 cells (ATCC; Rockville, MD) were cultured in DMEM/F12 media containing 5% fetal bovine serum and 1× penicillin/streptomycin. Human TRPA1 over-expressing HEK-293 cells were generated as previously described<sup>13,19</sup> and were cultured in DMEM:F12 media containing 5% fetal bovine serum, 1× penicillin/streptomycin, and geneticin (300 µg/mL). Human adenocarcinoma (A549) cells (ATCC; Rockville, MD) and lung fibroblast (IMR-90) cells were cultured in DMEM containing 5% FBS and 1× penicillin/streptomycin. (ATCC; Rockville, MD). Human lobar bronchial epithelial cells (Lobar; donor ID: 01344) were purchased from Lifeline Cell Technology (Frederick, MD). All primary cells were maintained for no more than 5 passages according to supplier recommendations.

**TRPA1/Ca<sup>2+</sup> Flux Assays.** Calcium imaging assays were performed in 96-well plates using the Fluo-4 Direct assay kit (Invitrogen) and an EVOS FL auto microscope (whole particles) or BMG Labtech NOVOSTar plate reader (particle extracts). Treatment-induced changes in cellular fluorescence were quantified using the average value for change in fluorescence, normalized to the maximum response elicited by ionomycin (10 µM).<sup>13,19</sup> In some instances, the data were also normalized to the prototypical TRPA1 agonist AITC.

Data were also corrected for nonspecific responses, if any, observed with HEK-293 cells. All agonist, particle, particle extract treatment solutions were prepared in LHC-9 containing 2% DMSO at a 3× concentration and added to cells at 37 °C. The final particle concentration indicated in the figures represents the concentration of the suspension (or extract) in the treatment well.

**TRPA1 Mutagenesis and Transient Over-Expression.** Human TRPA1 was cloned as previously described.<sup>13</sup> The TRPA1-ST mutant was generated using the QuickChange XL site-directed mutagenesis kit (Stratagene, La Jolla, CA). Transient transfection of HEK-293 cells with TRPA1 mutant plasmids was achieved using Lipofectamine 2000 (Invitrogen), also as described.<sup>13,19</sup>

**Acute Cytotoxicity Assay.** Cytotoxicity assays were performed on cells grown in 96-well plates and treated at 85–90% confluence (24–48 h after plating). Residual cell viability at 24 h was assessed using the Dojindo Cell Counting Kit 8 (Dojindo; Rockville, MD).

**qPCR Gene Expression.** A549, IMR-90, and Lobar cells were plated into 12-well plates. At 80% confluence, cells were treated with DEP extracts or DEP components. After 24 h, the cells were harvested and total RNA was isolated using the GenElute Mammalian Total RNA Miniprep Kit (Sigma; St. Louis, MO). Total RNA (1 µg) was converted to cDNA using iScript Reverse Transcription Supermix (BioRad; Hercules, CA). The cDNA was diluted 1:20 or 1:4 (IL-8 or MUC) for analysis by quantitative real-time PCR (qPCR) using a Life Technologies QuantStudio 6 Flex instrument and the TaqMan probe-based assays for human IL-8 (Hs00174103\_m1), MUC4 (Hs00366414\_m1), or MUC5B (Hs00861595\_m1). All values were normalized to  $\beta$ 2-microglobulin ( $\beta$ 2M; Hs00984230\_m1). Data are represented as percent change from vehicle control or DEP response and quantified using  $\Delta\Delta$ Ct.

**Mouse DEP Instillations, Histopathology, and Pulmonary Mechanics Measurements.** Male C57BL/6 mice (6–8 weeks old; ~20g) were anesthetized by intraperitoneal (i.p.) injection of ketamine plus xylazine (50 + 8 mg/kg) and treated with 3 doses of sterile saline (0.9%) or DEP suspended in saline at 0.5 mg/kg (25 µL total volume) every other day via oropharyngeal aspiration, with analysis 24 h after the third dose. Changes in baseline lung properties and sensitivity to methacholine challenge were then assessed using a Flexivent FX1 system (Scireq). Briefly, mice were anesthetized by i.p. injection of ketamine plus xylazine (100 + 16 mg/kg), paralyzed (0.1 mg/kg vecuronium bromide), and tracheostomized. Animals were constantly ventilated using the Flexivent system and the body temperature maintained using a circulating water heating pad. Parenchymal and airway resistance, tissue elastance, and compliance were measured at baseline and following serial methacholine challenge. Following assessment of pulmonary mechanics, the lungs were inflated with 10% neutral-buffered formalin at 25 cm H<sub>2</sub>O for 30 min, excised, placed in formalin overnight, and placed in 70% ethanol for processing at the University of Utah Research Histology Core. Hematoxylin and eosin stained (H&E) as well as periodic acid Schiff stained (PAS) sections were then evaluated for histopathological changes.

## RESULTS

**Pulmonary C-Fiber Activation.** “Black smoker” DEP was used as a model DEP and TRPA1 agonist to determine if a suspension of DEP could activate TRPA1-expressing C-fiber nerve terminals in the intact, uninjured lung. A total of 10 individual C-fibers were studied. All 10 C-fibers responded to capsaicin (end pulse of 1 µM), but only 7 of 10 responded to AITC. DEP (1 mg/mL, infused) weakly, but selectively, activated 4 of the 7 (57%) slow-conducting (0.45–0.58 m/s) AITC-sensitive C-fibers, but did not activate the 3 AITC-negative C-fibers. The average action potential peak discharge for AITC was 16.3±2.7 Hz, and the average action potential peak discharge for DEP was 1.7 ± 0.7 Hz (Figure 1). DMSO failed to evoke any response.

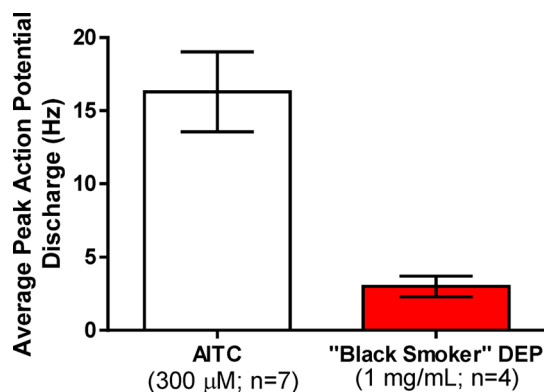


**Figure 1.** Average peak action potential discharge values for pulmonary C-fiber neurons stimulated with the TRPA1 agonist AITC (300 µM) or a suspension of “black smoker” DEP (1 mg/mL), perfused into lungs.

**DEP Potency.** DEP Potency was studied in TRPA1 over-expressing HEK-293 cells using calcium flux as a measure for TRPA1 activity. Whole-particle emission station DEP was the most potent TRPA1 agonist, followed by “black smoker,” NIST SRM 2975, and regenerated filter DEP (Figure 2A). The relative potency of the DEP samples appeared related to the ability of the PM to interact with the cells, and TRPA1 activation was generally correlated with the mean hydrodynamic radii of the DEP ( $R^2 = 0.7766$ ;  $p = 0.2234$ ) and suspension stability. Accordingly, TRPA1 activation was found to be directly proportional to the percentage of extractable material obtained from the various DEP samples: emission station DEP was  $\sim 32 \pm 1\%$  extractable using ethanol, “black smoker” was  $\sim 30 \pm 4\%$ , NIST SRM 2975 was  $\sim 9 \pm 1\%$ , and regenerated filter DEP was  $\sim 0.7 \pm 0.2\%$  (Figure 2B). Correlation analysis of TRPA1 potency versus percent extractable mass yielded an  $R^2$  value of 0.9423 ( $p = 0.0293$ ). To this end, when particle extract residues were compared on an equal mass basis, equivalent potency was observed (Figure 2C), suggesting that particle bound and leachable chemicals were responsible for TRPA1 activation.

**Characterization of DEP Size, Shape, and Elemental Composition.** The physical and elemental characteristics of the four DEP were assayed by SEM and EDS. Aggregates of all four DEP were similar sponge-like loosely aggregated carbonaceous soot (Figure 3A). The “black smoker” and NIST SRM 2975 DEP were primarily carbon, but trace quantities of Al, Si, and S were present in the “black smoker” DEP. The emissions station DEP contained the highest quantities of Si > Fe > Cl > S > Al, Ca, and P with multiple micron to submicron iron-rich particles associated with the soot (Figure 3B). The regenerated filter DEP resembled the emissions station DEP, but with lower levels of trace minerals and metals, and no evidence of iron-rich particles (Figure 3A).

**Chemical Analysis of DEP.** The chemical composition of the extracts obtained from the DEP samples was initially evaluated by high-resolution GC–MS and PCA analysis of the spectral data; chromatograms are shown in Supplemental Figure 1. The PCA loading plot (Figure 4A) indicated substantial differences in the chemical makeup of the DEP samples. The emissions and “black smoker” DEP were chemically distinct from each other as well as both the NIST SRM 2975 and the regenerated filter DEP. The NIST SRM 2975 and the regenerated filter DEP were chemically similar,



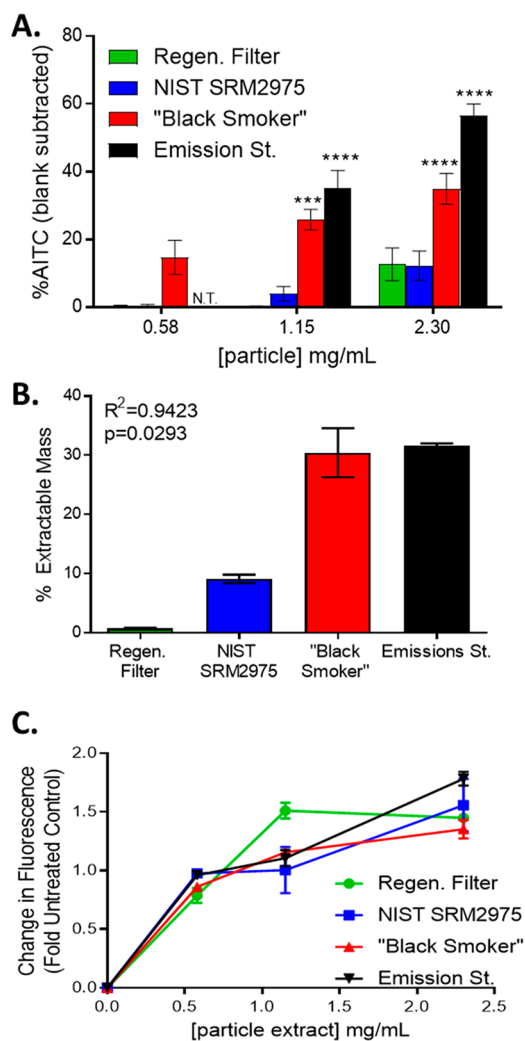


**Figure 2.** (A) Activation of human TRPA1 (cellular  $\text{Ca}^{2+}$  influx) by equivalent concentrations of DEP suspended in treatment media using HEK-293 cells stably overexpressing the human TRPA1 channel and loaded with the fluorogenic calcium indicator Fluo-4AM. (B) Ethanol extractable content of the four DEP samples. (C) Activation of TRPA1 by equivalent masses of ethanol extracted DEP residues using HEK-293 cells stably overexpressing the human TRPA1 channel and loaded with the fluorogenic calcium indicator Fluo-4AM. N.T.: not tested. Single asterisks indicate a significant increase in calcium flux relative to HEK-293 treated controls (triple asterisks indicate  $p < 0.005$ ; quadruple asterisks indicate  $p < 0.0001$ ) using a two-way ANOVA with Bonferroni multiple comparisons test.

albeit differences in specific chemical constituents were observed. Figure 4B shows a comparison of polycyclic aromatic hydrocarbons (PAHs) and several other chemicals among equivalent quantities of extracted mass from the four DEP samples. The "black smoker" DEP had the highest abundance of PAHs, followed by the NIST SRM 2975 DEP. Substantially lower quantities of PAHs were in the emissions station and regenerated diesel filter samples, which presumably contained more elemental carbon.

**TRPA1 Activation by DEPs.** Electrophilic agonists of TRPA1 bind to C621, C641, C665, and K710 residues (3CK site) on the intracellular N-terminal portion of TRPA1, which can be inhibited by pretreating particles or extracts with glutathione (GSH) to effectively reduce the concentration of electrophiles available to activate TRPA1. Common among the

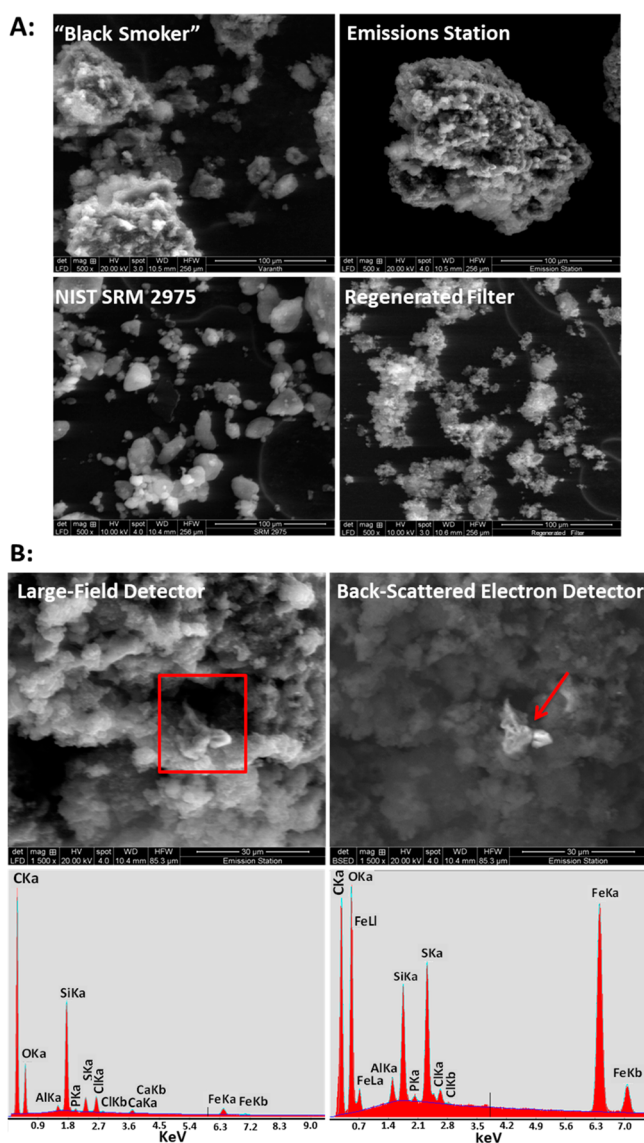


**Figure 3.** (A) Scanning electron micrograph (SEM) images (500 $\times$ ) of the four DEP samples used as TRPA1 agonists. (B) Comparison of SEM images of emissions station DEP using (left) a large field detector or (right) back-scattered electron detector showing the presence of an electron dense iron-rich particle associated with the larger soot material. Below are the representative screen-capture images from EDS analysis of the emissions station DEP, showing the enrichment of iron associated with the highlighted (red arrow) small particle associated with the soot.

DEP samples were the electrophilic TRPA1 agonists 1,2- and 1,4-naphthoquinone, benzoquinone, and perinaphthenone and the non-electrophilic TRPA1 agonist 2,4-ditert butylphenol. 3EPPB, which we previously identified as a TRPA1 agonist,<sup>13</sup> was also present at variable concentrations. The peak areas of these chemicals in equivalent masses of the DEP extracts, and the relative percentage of these chemicals in the respective extracts are shown in panels C and D of Figure 4, respectively. Activation of TRPA1 by perinaphthenone was significantly inhibited by GSH pretreatment and was unaffected by mutation of the menthol/ST binding site, which is the target of multiple known nonelectrophilic TRPA1 agonists. Conversely, TRPA1 activation by 3EPPB and 3,5-ditert butylphenol (an analogue of 2,4-ditert butylphenol also found in some

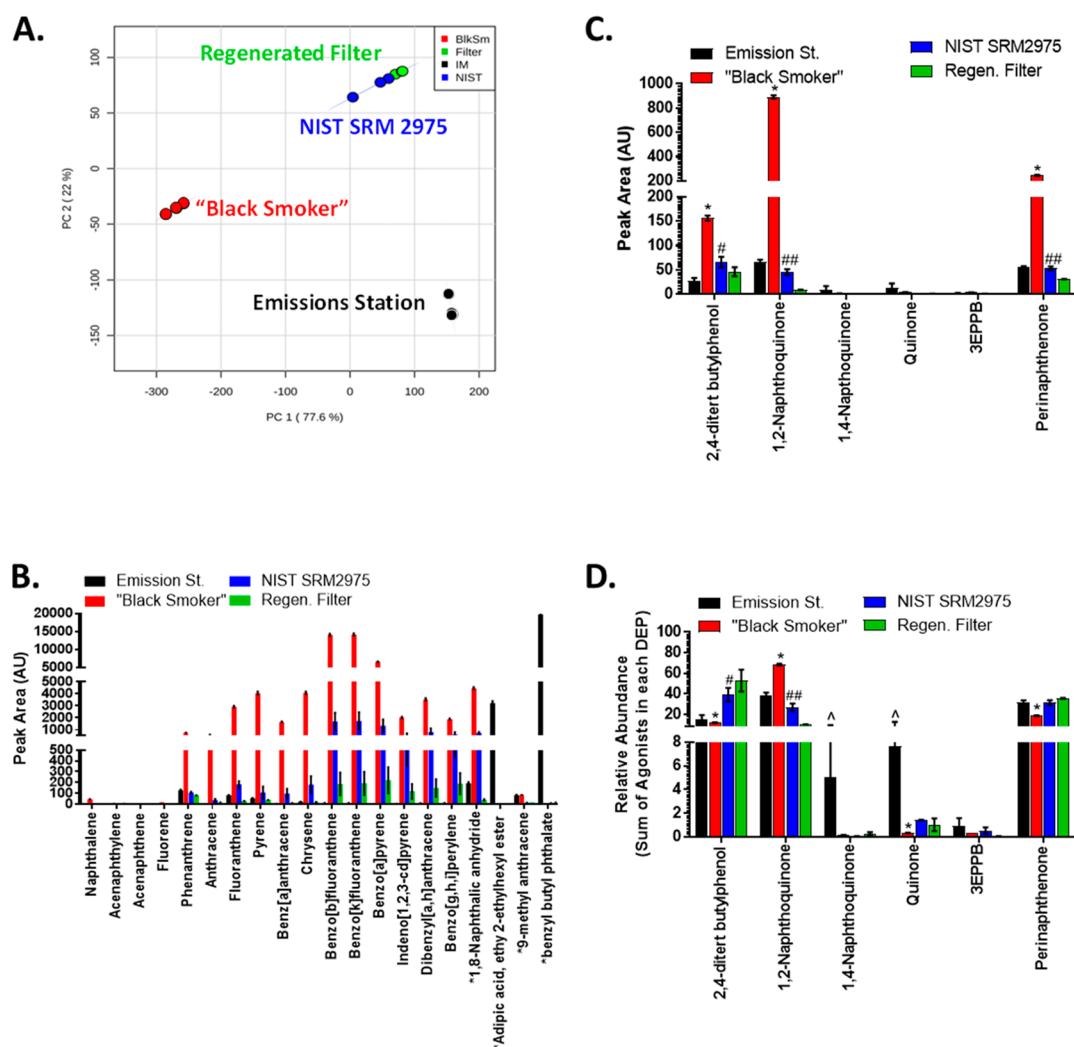


**Figure 4.** (A) PCA plot comparing the chemical composition of equal masses (1.0 mg) of ethanol extracts from the four DEP samples. The plot was generated using Metaboanalyst software. (B) Results showing the average GC–MS peak areas of 17 PAHs and 3 additional preliminarily identified compounds (by spectral data similarity) in equivalent masses of extract for the four DEP samples. (C) GC–MS peak area values of known TRPA1 agonists in extracts of the four DEP samples. Single asterisks indicate that the “black smoker” was greater than all other DEP ( $p < 0.001$ ). A single pound sign indicates NIST SRM2975 was greater than the emissions station; double pound sign indicate NIST was greater than regenerated filter DEP ( $p < 0.01$ ). The two-way ANOVA with Bonferroni multiple comparisons test was used. (D) Relative abundance of specific TRPA1 agonists in a given extract material, normalized to the sum of all agonist peak areas in a given sample. Single asterisks indicate that “black smoker” was greater or lower than all other DEP ( $p < 0.001$ ). Single pound signs indicate that NIST SRM2975 was greater or less than the emissions station. Carats indicate that the emissions station DEP was greater than all others ( $p < 0.001$ ). The two-way ANOVA with Bonferroni multiple comparisons test was used.

DEP) was unaffected by GSH pretreatment, but significantly inhibited by mutation of the menthol/ST binding site (Figure 5A).

1,2- and 1,4-Naphthoquinone, benzoquinone, perinaphthenone, 2,4-ditert butylphenol, and 3EPPB were most abundant in the “black smoker” DEP sample (Figure 4C). However, the relative abundance of these compounds varied among the four DEP samples (Figure 4D). 2,4-Ditert butylphenol and perinaphthenone were among the most abundant chemicals on a residue mass basis in the regenerated filter DEP sample (~3–5%), whereas benzoquinone and 1,2-naphthoquinone were more abundant in the emissions station, “black smoker” and NIST SRM 2975 samples. TRPA1 activation by “black smoker” and regenerated filter DEP extracts was inhibited by both GSH pretreatment and mutation of the menthol/ST binding site. Activation by NIST SRM 2975 was only inhibited

by GSH pretreatment, while emissions station diesel was primarily inhibited by mutation of the menthol/ST binding site (Figure 5B). Of note, TRPA1 was not acutely activated in calcium flux assays by the PAHs naphthalene or phenanthrene,<sup>13</sup> benzo[a]pyrene (up to 250  $\mu$ M), or the mixture of PAHs used as the analytical standard for PAH analysis at a concentration of up to 0.25 mg/mL (data not shown). Overall, it is the relative abundance and bioavailability of the different TRPA1 agonists that appears to drive the mechanism of TRPA1 activation.

**Cytotoxic Properties of the DEP.** The impact of variable activation of TRPA1 by the different DEP samples and selected chemical constituents thereof on the acute cytotoxicity of the DEP and DEP extracts was evaluated using A549 and IMR-90 lung cells. These cells are representative lung cell types that expresses TRPA1 and which have been used in numerous

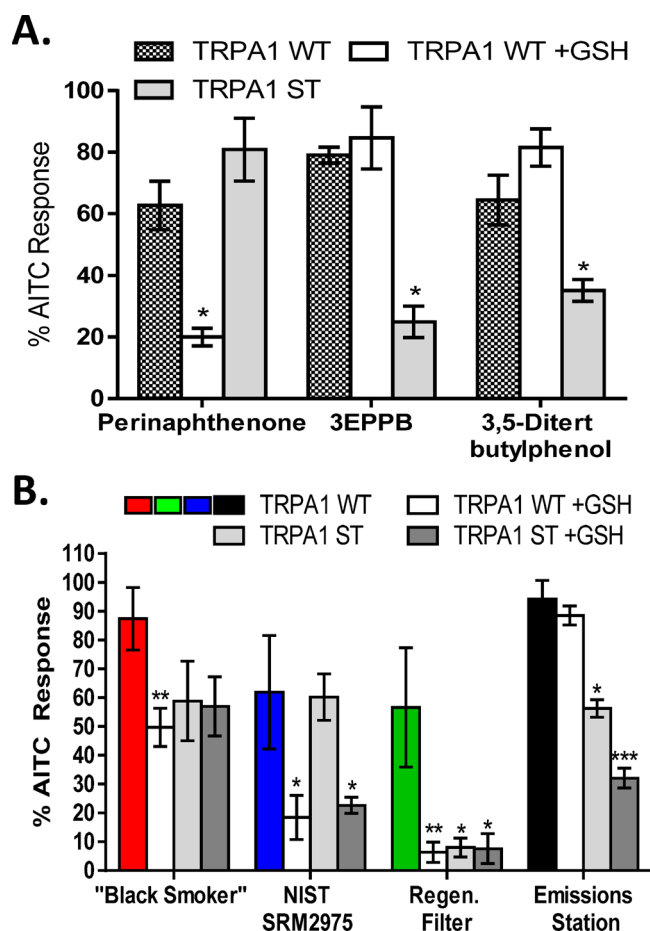


**Figure 5.** (A) Activation of TRPA1 and TRPA1 mutants by selected TRPA1 agonists (250  $\mu$ M) with and without GSH pretreatment in TRPA1-over-expressing HEK-293 cells loaded with Fluo-4. Results are normalized to the response of cells to AITC (200  $\mu$ M). Single asterisks indicate the significant inhibition ( $p < 0.05$ ) of the response by cells expressing the menthol-binding site mutant TRPA1-S873 V/T874L or using glutathione pretreatment (20 mM; 10 min) of the agonist prior to application to cells using two-way ANOVA with Bonferroni multiple comparisons test. (B) Activation of TRPA1 by ethanol extracted residues of "black smoker" (1.0 mg/mL), NIST SRM 2975 (2.3 mg/mL), emissions station (1.0 mg/mL), and regenerated filter DEP (2.3 mg/mL) and differential inhibition of the responses in TRPA1-S873V/T874L-expressing cells, upon GSH pretreatment of the DEPs, or both. Single asterisks indicate significant inhibition ( $p < 0.05$ ) using the two-way ANOVA with Bonferroni multiple comparisons test.

studies of DEP toxicity.<sup>16,19–22</sup> In A549 cells, the  $LC_{50}$  values for the extracts of the "black smoker," NIST SRM 2975, and regenerated filter DEP were equivalent ( $\sim 0.3$  mg/mL following a 24 h treatment; data not shown). Similar results were observed when using DEP suspensions in IMR-90 cells suggesting that TRPA1 activation is not paramount for acute cytotoxicity. The DEP components 1,2-naphthoquinone, benzoquinone, perinaphthenone, 2,4-ditert butylphenol, and 3EPPB exhibited  $LC_{50}$  values of 44, 14, 61, 41, and 29  $\mu$ M, respectively, in A549 cells. However, like for the DEP and extracts, the relative potency of these substances as TRPA1 agonists was not predictive of the relative cytotoxicity of these substances.

**Pro-Inflammatory Properties of the DEP.** Induction of the commonly studied pro-inflammatory gene IL-8 was also

evaluated in A549 and IMR-90 cells. "Black smoker" DEP extract (0.64 mg/mL) and the electrophilic component perinaphthenone (40  $\mu$ M;  $LD_{50} = 61$   $\mu$ M) failed to induce IL-8 in A549 cells despite being TRPA1 agonists (Figure 6A,B). Conversely, 4- and 15-fold induction of IL-8 was observed with an equivalent concentration of the extract of the regenerated filter DEP sample and 2,4-ditert butylphenol ( $LD_{50} = 41$   $\mu$ M), with the effect of the regenerated filter DEP extract being inhibited  $\sim 60\%$  by co-treatment of cells with the TRPA1 antagonist HC-030331 (20  $\mu$ M) (Figure 6A,B); the lack of inhibition of 2,4-ditert butylphenol-induced IL-8 mRNA induction is likely due to the expression of TRPV3 in A549s, which is also activated by this compound.<sup>23</sup> In IMR-90 cells, which we found to not express TRPV3, the rank order for potency for IL-8 mRNA induction for the DEP extracts was regenerated filter > emissions station > NIST SRM 2975 > "black smoker DEP". In IMR-90 cells, the TRPA1 antagonist HC-030031 also substantially inhibited IL-8 mRNA induction by the filter, emissions station, and NIST DEP, as well as 2,4-ditert butylphenol (Figure 6C,D), further supporting the proposed role for TRPV3 in mediating the response to 2,4-ditert butylphenol and certain forms of DEP in A549 cells.

**Pulmonary Effects of DEPs.** The relative pneumotoxicity of the "black smoker," NIST SRM 2975, and regenerated filter DEP (i.e., three distinct TRPA1 agonists) were further compared in mice following subacute oropharyngeal dosing. Mild inflammatory responses were observed with all three DEP. Where particles were observed, particle-laden macrophages, occasional leukocytes (mainly neutrophils), slightly thickened alveolar septa, and basophilic exudates were observed; however, these effects varied between the three DEP tested. Figure 7A,C,E shows H&E-stained sections highlighting the epithelium of a large diameter airway of a mouse treated with "black smoker," regenerated filter, and NIST SRM 2975 DEP, respectively. Enhanced mucous production and goblet cell metaplasia was also readily evident in mice treated with the "black smoker" (Figure 7B) and regenerated filter DEP (Figure 7D) (PAS; arrows show enhanced staining), but not with NIST SRM 2975 (Figure 7F). Consistent with the results for mucin production in mouse airways, the induction of mucin 4 and 5B, but not 5AC, was observed in primary human lobar bronchial epithelial cells treated with regenerated filter DEP, which was partially attenuated by the TRPA1 antagonists HC-030031 and A967079 (Figure 7G,H). Finally, in the distal airways and alveolar region, accumulation of particles in macrophages was observed for all three DEP (Figure 8A–F; arrows), where panels A and B are from "black smoker"-treated mice, panels C and D are from regenerated filter-treated mice, and panels E and F are from NIST SRM2975-treated mice. However, despite these differential effects, particularly in mucous secretion, no significant differences in pulmonary mechanics (i.e., baseline resistance, compliance, or elastance) or hypersensitivity to aerosolized methacholine were observed between saline, "black smoker" DEP, NIST SRM 2975, or the regenerated filter DEP-treated groups (Supplementary Figure 2).

## DISCUSSION

The effects of DEP in *in vitro* and in animal models can vary widely as a function of the DEP source, cell types, and animal models used. With respect to DEP, engine operating conditions, fuel type, age, collection methods, etc. impact



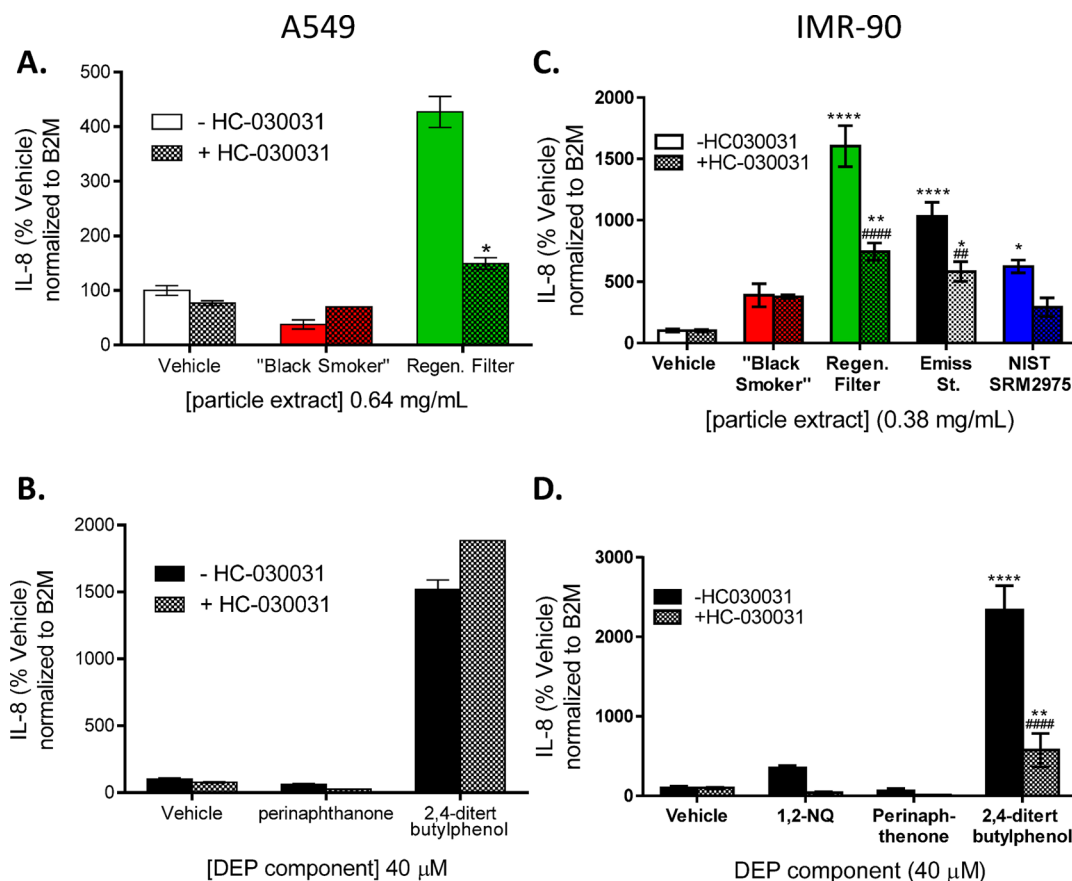


**Figure 6.** (A) Expression of IL-8 mRNA in A549 cells treated with either a vehicle control, "black smoker," or regenerated filter DEP extracts (0.64 mg/mL) for 4 h in the presence or absence of the TRPA1 antagonist HC-030031 (20  $\mu$ M). (B) Expression of IL-8 mRNA in A549 cells treated with either a vehicle control, 1,2-naphthoquinone (40  $\mu$ M) or 2,4-ditert butylphenol (40  $\mu$ M) for 4 h in the presence or absence of the TRPA1 antagonist HC-030031 (20  $\mu$ M). Asterisks indicate significant induction relative to the control group ( $p < 0.05$ ) using the two-way ANOVA with Bonferroni multiple comparisons test. (C, D) Changes in IL-8 mRNA expression in IMR-90 cells as above but at (0.38 mg/mL). Single asterisks indicate significant induction relative to the control, while pound symbols signify the inhibition of induction using the TRPA1 antagonist HC-030031 ( $p < 0.05$ ) using the two-way ANOVA with Bonferroni multiple comparisons test.

particle compositions. Variation in biological effects of DEP is undoubtedly related to differences in physical and chemical properties, which can be further complicated by the presence, absence, and relative engagement of biologically important molecular targets in a given test system. The effect of DEP composition was illustrated, for example, by Singh et al.,<sup>22</sup> who reported that automobile DEP (A-DEP) and NIST SRM 2975 DEP varied in physical structure and organic and elemental carbon content, which translated into variations in pulmonary inflammatory effects: Specifically, differential induction of IL-5, TNF $\alpha$ , MIP-2, *N*-acetyl- $\beta$ -D-glucosaminidase, total antioxidant capacity, and the relative influx of total polymorphonuclear (PMN) cells and macrophages was observed, while IL-6 and extravasated microalbumin were similar.

This study further explored the hypothesis that differences in the activation of TRPA1 by environmental particles such as DEP may represent a mechanistic basis for variable responses to complex particulate materials by lung cells. We used multiple forms of DEP having different relative potency, chemical composition, and mechanisms of TRPA1 activation to address this hypothesis. To summarize, the answers to the five questions posed in the introduction were essentially "yes" in all cases, but certainly not without caveats.

The first question asked was: Can TRPA1-expressing C-fibers be activated by a representative DEP suspension in the

intact, uninjured lung? "Black smoker" DEP, which was among the most-potent DEP, evoked action potentials from AITC-sensitive bronchopulmonary C-fiber nerve terminals (Figure 1). Although limited in discharge frequency, these DEP-induced responses were restricted to TRPA1-expressing fibers. As such, suspended solid DEP such as the "black smoker" DEP, and presumably, other forms of DEP with comparable potency and chemical properties (e.g., emissions station DEP), can activate TRPA1 in airway sensory neurons without the need of epithelial disruption. While this assay does not fully replicate inhalation exposure to DEP, these findings agree with other studies indicating a TRPA1- and C-fiber-mediated effect on cardiovascular function in rats exposed to diesel exhaust.<sup>24</sup>

The second question asked was: Would TRPA1 be uniquely activated by different types of DEP? Indeed, all four forms of DEP were agonists of TRPA1 (Figure 2A), but the relative potency of the materials varied significantly. There were three criteria that appeared to impact the potency of DEP at TRPA1: (1) particle settling onto cells, (2) the percentage of ethanol extractable polar organic chemicals (i.e., bioavailability of chemical agonists), and (3) the types and relative amounts of TRPA1 agonists associated with the DEP, with the latter seemingly being the most important driver of differences in biological responses to the DEPs. Rapidly settling and highly extractable DEP exhibited the greatest potency. However,

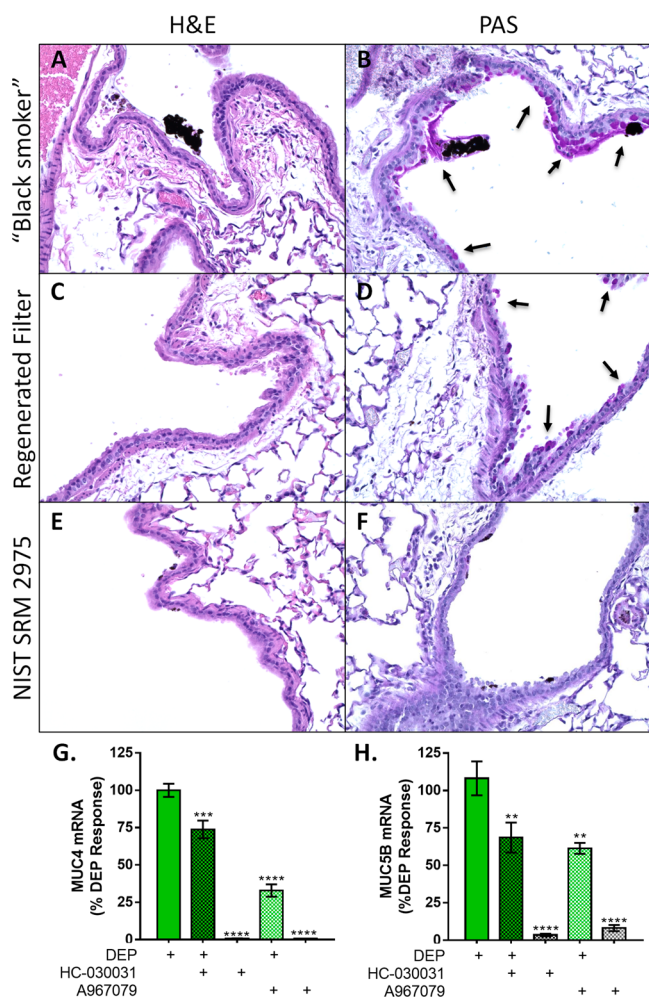


**Figure 7.** Representative photomicrographs of H&E (panels A, C, and E) and PAS (panels B, D, and F) lung tissue from mice collected after treatment with “black smoker” (panels A and B), regenerated filter (panels C and D), or NIST SRM 2975 DEP (panels E and F). The images were captured at 40 $\times$  using an EVOS FL auto imaging system. (G, H) Relative expression of mRNA for mucin 4 and 5B (MUC4 and MUC5B) by primary human lobar bronchial epithelial cells treated with regenerated filter DEP for 24 h in the presence or absence of the TRPA1 antagonists HC-030031 (20  $\mu$ M) or A967079 (20  $\mu$ M). Double asterisks indicate significant inhibition relative to DEP induced mucin mRNA ( $p < 0.01$ ) using the one-way ANOVA with Bonferroni’s multiple comparison test.

equivalent potency was achieved by treating cells with an equal mass of extracted material (Figure 2B) indicating that liberation of TRPA1 agonists and concentrating them can promote TRPA1 activation. This characteristic has also been reported by others using a variety of end points, including Singh et al.,<sup>22</sup> who demonstrated differences in biological effects presumably related to extractable PAH content.

The third question asked whether the biochemical mechanism of TRPA1 activation would vary as a function of the chemical composition of the DEP. Using SEM, it was found that all four DEP were aggregates of soot with similar shape. The subtle differences observed in the powdered forms did not inform us of physical criteria that may account for the observed differences in potency in the biological assays (Figures 2A and 3A), although there was a loose correlation between particle size and settling rates and activation of TRPA1. However, using EDS, it was found that the emission

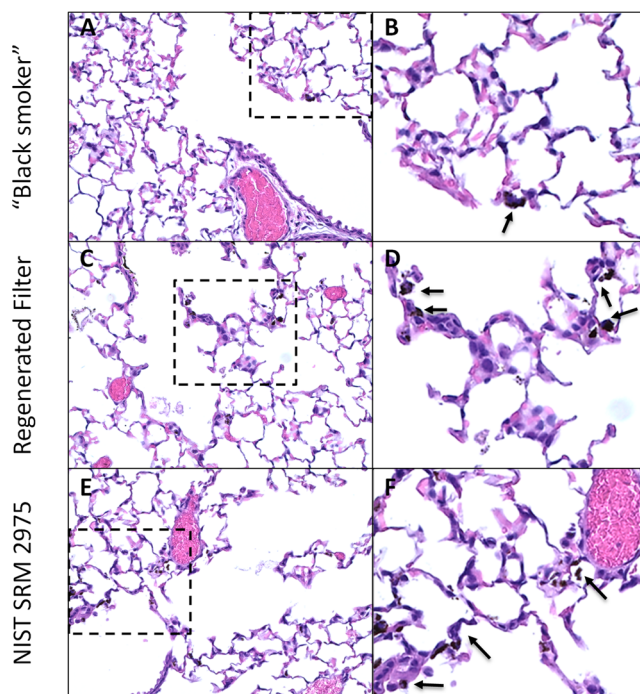


**Figure 8.** Representative photomicrographs of H&E-stained distal airway tissue from mice collected after treatment with “black smoker” (panels A and B), regenerated filter (panels C and D), or NIST SRM 2975 DEP (panels E and F). Panels A, C, and E were captured at 40 $\times$  using an EVOS FL auto imaging system. Panels B, D, and F are expanded from the corresponding images to the left, as indicated by the box.

station DEP contained numerous small iron-rich particles embedded in the soot material (Figure 3B). Iron catalyzes redox reactions in aerobic aqueous solutions in the presence of reductants, a condition that exists in cell culture media. Thus, iron may have also contributed to the high potency of the emission station diesel through the generation of extracellular H<sub>2</sub>O<sub>2</sub>, which would not be affected by GSH pretreatment, but could promote the formation of cellular oxidative breakdown products that can activate TRPA1.<sup>25–27</sup> This idea was supported by the finding that the activation of TRPA1 by emissions station DEP extract was partially attenuated by GSH pretreatment, but only in TRPA1-ST mutant cells, where the contribution of co-occurring electrophilic and nonelectrophilic chemical TRPA1 agonists was mitigated (Figure 5B). An alternative interpretation is that the response to this DEP was near saturation when both TRPA1 activation sites were engaged. Regardless, simply assessing DEP size and shape was not sufficient to predict TRPA1 agonist activity, or to explain the observed differences in biological effects elicited by the DEPs.

The DEP were also analyzed for chemical variation using an indiscriminant GC–MS approach and PCA (Figure 4A). The emissions station and “black smoker” DEP were chemically distinct, while the NIST and regenerated filter samples were similar. The quantitation of 17 different PAHs and other chemicals was performed. The PAH content was highest in the “black smoker” DEP, similar to the automobile DEP sample used by Singh et al.<sup>22</sup> Conversely, the emissions station DEP was low in PAHs like the NIST SRM 2975 and regenerated filter DEPs, but contained numerous phthalates of unknown origin. These differences were key drivers of the PCA results,



Table 1. Summary of DEP and DEP Extract Effects on TRPA1 and Toxicological End Points

DEP sample		TRPA1 (Ca <sup>++</sup> flux)	activation site	TRPA1 agonists	*PAH content	IL-8 induction	PAS staining
black smoker	particle	+++	N.T.	1,2-NQ>> perinaphthenone>> 2,4-DTBP	++++	N.T.	++
	extract	++++	3CK+ST			+	N.T.
emissions station	particle	++++	N.T.	1,2- and 1,4-NQ> perinaphthenone = 2,4-DTBP >	+	N.T.	N.T.
	extract	++++	ST	quinone		+++	N.T.
NIST SRM 2975	particle	++	N.T.	2,4-DTBP> perinaphthenone = 1,2-NQ	+++	N.T.	N.D.
	extract	++	3CK			++	N.T.
regenerated filter	particle	+	N.T.	2,4-DTBP> perinaphthenone>> 1,2-NQ	++	N.T.	+
	extract	+	3CK=ST			++++	N.T.

<sup>a</sup>N.T. = not tested; N.D. = none detected. Asterisks indicate likely to require bioactivation to, e.g., quinones. <sup>b</sup>1,2-NQ, 1,2-naphthoquinone; 2,4-DTBP, 2,4-*ditert* butylphenol.

but were not necessarily the basis for differences in TRPA1 activation. TRPA1 was not acutely activated in calcium flux assays by any of the PAHs or phthalates tested, consistent with prior results reported by our group.<sup>13</sup> Albeit, compounds such as naphthalene can undergo cytochrome P450 mediated bioactivation to produce 1,2-naphthoquinone, which potently activates TRPA1.<sup>28</sup> Regardless, the striking differences in PAH content between the “black smoker” DEP and the other DEPs did not correlate with TRPA1 activation, but could explain reported differences in the ability of DEP samples to induce AhR signaling, cellular changes in lungs (i.e., macrophages versus PMN)<sup>22</sup> and CYP1A/1B enzyme induction as well as tumorigenesis.<sup>28</sup> These specific end points were not studied here, but differences in the induction of IL-8 in A549 and IMR-90 cells was observed (Figure 6A–D), and slightly higher levels of macrophages were observed in lung lavage fluid (not shown) from mice treated with the PAH-rich “black smoker” DEP compared to the NIST SRM 2975 (intermediate PAHs) and regenerated filter DEP (low PAHs) (Figures 7 and 8). Additionally, “black smoker” DEP stimulated mucous production to the largest degree (Figure 7B,D,F), which, in cultured human lung cells, was partially TRPA1-dependent (Figure 7G,H). In general, these results agree with those reported by Singh et al.<sup>22</sup> and show that the chemical composition of DEP can have substantial effects on how lung cells respond to exposure, which may be, in part, through activation of TRPA1 by specific chemical entities.

Known TRPA1 agonists were also quantified in the four DEP samples by either GC–MS or LC–MS/MS, including analysis of dinitrophenylhydrazine conjugates, as previously described.<sup>13,19</sup> Figure 4C,D shows that the “black smoker”, emissions station, and NIST SRM 2975 DEP were rich in electrophilic TRPA1 agonists, namely 1,2- and 1,4-naphthoquinone, quinone, and perinaphthenone. Conversely, the regenerated particle filter DEP, which is subjected to repeated intense heating in the particle filter and during filter regeneration, had lower quantities of electrophiles (e.g., 1,2- and 1,4-naphthoquinone), but relatively high quantities of the nonelectrophilic TRPA1 agonist 2,4-*ditert* butylphenol, which was present at lower relative quantities in the other DEP.

The activity of perinaphthenone as a TRPA1 agonist was confirmed to involve the electrophile sensor of TRPA1, based on inhibition by pretreating the agonist with GSH (Figure 5A), similar to other electrophiles.<sup>19</sup> The activity of 3,5-*ditert* butylphenol (an equipotent analogue of 2,4-*ditert* butylphenol) was also confirmed to involve the menthol/ST binding site. Novel was that 3EPPB also activated TRPA1 through the menthol/ST binding site. Consistent with these results, the

mechanism by which TRPA1 was activated by the various DEP materials varied as a function of the relative quantities of the electrophilic and nonelectrophilic agonists present, and their relative potency. For example, “black smoker” DEP contained 2,4-*ditert* butylphenol and the potent electrophilic TRPA1 agonist 1,2-naphthoquinone. TRPA1 activation by extracts of the “black smoker” DEP was inhibited by both GSH pretreatment and with mutation of the menthol/ST binding site, albeit to a lesser extent (Figure 5B). Conversely, extracts of the regenerated filter DEP sample activated TRPA1 equally via both the electrophile and menthol/ST binding sites, presumably dominated by the potent nonelectrophilic agonist 2,4-*ditert* butylphenol. Thus, the relative proportion and potency of agonists present on a given particle or in a particle extract impact how these materials interact with the TRPA1 channel to affect cellular responses.

The fourth question was: Would variations in TRPA1 activation by different forms of DEP translate into differences in commonly observed cellular responses to DEP treatment (e.g., cytokine gene induction) in lung cell lines known to express TRPA1? The answer is yes. A549 and IMR-90 cells express TRPA1 and were used here as a model for lung epithelial cells that express TRPA1.<sup>16,19–22</sup> There were no differences in the cytotoxicity of the DEP extracts despite having different relative chemical compositions. However, the regenerated filter DEP extract sample was substantially more potent at inducing IL-8 than the “black smoker” DEP extract, which, surprisingly, did not occur to a significant level in either A549 or IMR-90 cells (Figure 6A,C). Furthermore, the induction of IL-8 by the regenerated filter DEP extract sample was inhibited by the TRPA1 antagonist HC-030031 in A549 cells and, similarly, for NIST SRM, filter, and emissions station DEP extracts in IMR-90 cells. However, the difference in IL-8 induction by these materials and chemicals was initially puzzling, given numerous reports that treatment of lung cells with DEP almost universally induces this gene. Hence, this disparity was further explored. In results that are not shown, it was found that calcium flux, a marker of TRPA1 activation in A549 cells and precursor to IL-8 induction, was not observed for perinaphthenone or 1,2-naphthoquinone despite being observed with AITC and 2,4-*ditert* butylphenol. A549 cells are known to have a mutated NRF2:KEAP1 system, leading to constitutive activity and extensive up-regulation of antioxidant defenses.<sup>29,30</sup> This cell-specific factor may interfere with TRPA1 activation by some electrophiles, partially explaining the differences in IL-8 induction between “black smoker” DEP and the regenerated filter sample, and may highlight a basis explaining the often reported variability in pro-inflammatory

potency of different DEPs in A549 cells. However, the hypothesis regarding NRF2:KEAP1 does not necessarily apply to IMR-90 cells, and IMR-90 cells do not appear to express TRPV3 as A549s do. As such, more work is needed to fully understand this finding.

The fifth question asked was: Would variations in TRPA1 activation by DEP promote differences in lung inflammation or injury in mice? Indeed, differences in cellular infiltrates, mucous secretion, and goblet cell metaplasia were observed in mouse airways treated with different DEP. Consistent with the IL-8 results in Figure 6, the regenerated filter DEP appeared to induce a more-robust PMN response compared to the “black smoker” DEP, but the BAL analysis results were not statistically significant. However, the overall impact of the DEP in mouse lungs was mild, making highly significant comparisons using more quantitative histopathological and functional criteria difficult. In a similar manner, no significant differences were observed for pulmonary mechanics measurements (Supplementary Figure 2).

In summary, this study illustrates that TRPA1 is activated on airway C-fibers in an intact lung model and in multiple cultured human lung cell models by a variety of qualitatively and quantitatively different DEP, but with different potencies and chemical mechanisms, as summarized in Table 1. While TRPA1 likely contributes to the pro-inflammatory effects of particles like DEP in the respiratory tract via both neurogenic and non-neurogenic pathways, pulmonary inflammatory responses are clearly very complex and do not appear to be easily explained by comparing the potency or mechanism of activation of TRPA1. Thus, it is likely that the molecular differences that occur in response to different DEP are only partially mediated by TRPA1. One example could include the involvement of TRPV3, as suggested by results for IL-8 induction in Figure 6B. Finally, this study further emphasizes the importance of ascertaining both particle and model/cell-specific properties that drive end-point effects because they will undoubtedly affect experimental outcomes and associated mechanistic conclusions.

## ■ ASSOCIATED CONTENT

### 📄 Supporting Information

The Supporting Information is available free of charge on the ACS Publications website at DOI: [10.1021/acs.chemrestox.8b00375](https://doi.org/10.1021/acs.chemrestox.8b00375).

Figures showing a high-resolution GC–MS chromatograms of 4 different DEPs and pulmonary mechanics measurements from mice treated with 3 types of DEP (PDF)

## ■ AUTHOR INFORMATION

### Corresponding Author

\*E-mail: [chris.reilly@pharm.utah.edu](mailto:chris.reilly@pharm.utah.edu); phone: (801)-581-5236.

### ORCID

Cassandra E. Deering-Rice: [0000-0002-2103-1194](https://orcid.org/0000-0002-2103-1194)

Christopher A. Reilly: [0000-0002-5006-1982](https://orcid.org/0000-0002-5006-1982)

### Notes

The authors declare no competing financial interest.

## ■ ACKNOWLEDGMENTS

This work was supported by NIH grant nos. ES017431 and ES027015. The SEM and EDS work made use of University of

Utah shared facilities of the Micron Microscopy Suite sponsored by the College of Engineering, Health Sciences Center, Office of the Vice President for Research, and the Utah Science Technology and Research (USTAR) initiative of the State of Utah.

## ■ ABBREVIATIONS

AITC, allyl-isothiocyanate; DEP, diesel exhaust particles; HEK-293, human embryonic kidney-293 cells; LHC-9, Lechner and LaVeck media; PM, particulate matter; SRM, Standard Reference Material; TRPA1, transient receptor potential ankyrin-1; TRPM8, transient receptor potential melastatin-8; TRPV1, transient receptor potential vanilloid-1; TRPV2, transient receptor potential vanilloid-2; TRPV3, transient receptor potential vanilloid-3; TRPV4, transient receptor potential vanilloid-4; 3EPPB, [(3E)-1-phenyl-1,3-pentadieny]benzene; HC-030031, 1,2,3,6-tetrahydro-1,3-dimethyl-N-[4-(1-methylethyl)phenyl]-2,6-dioxo-7H-purine-7-acetamide; A967079, (1E,3E)-1-(4-fluorophenyl)-2-methyl-1-penten-3-one oxime; 1,2-NQ, 1,2-naphthoquinone; 2,4-DTBP, 2,4-ditert butylphenol

## ■ REFERENCES

- (1) Hammond, D. M., Dvonch, J. T., Keeler, G. J., Parker, E. A., Kamal, A. S., Barres, J. A., Yip, F. Y., and Brakefield-Caldwell, W. (2008) Sources of ambient fine particulate matter at two community sites in Detroit, Michigan. *Atmos. Environ.* 42, 720–732.
- (2) Mauderly, J. L. (2010) Current Status of the Toxicology of Diesel Engine Exhaust - and the ACES Project. *Zentralbl. Arbeitsmed., Arbeitsschutz Ergon.* 60, 412–417.
- (3) Hazari, M. S., Haykal-Coates, N., Winsett, D. W., Krantz, Q. T., King, C., Costa, D. L., and Farraj, A. K. (2011) TRPA1 and Sympathetic Activation Contribute to Increased Risk of Triggered Cardiac Arrhythmias in Hypertensive Rats Exposed to Diesel Exhaust. *Environ. Health Perspect.* 119, 951.
- (4) Venkatachalam, K., and Montell, C. (2007) TRP Channels. *Annu. Rev. Biochem.* 76, 387–417.
- (5) Voets, T., Talavera, K., Owsianik, G., and Nilius, B. (2005) Sensing with TRP channels. *Nat. Chem. Biol.* 1, 85–92.
- (6) Vriens, J., Appendino, G., and Nilius, B. (2009) Pharmacology of Vanilloid Transient Receptor Potential Cation Channels. *Mol. Pharmacol.* 75, 1262–1279.
- (7) Caceres, A. I., Brackmann, M., Elia, M. D., Bessac, B. F., del Camino, D., D'Amours, M., Witek, J. S., Fanger, C. M., Chong, J. A., Hayward, N. J., Homer, R. J., Cohn, L., Huang, X., Moran, M. M., and Jordt, S. E. (2009) A sensory neuronal ion channel essential for airway inflammation and hyperreactivity in asthma. *Proc. Natl. Acad. Sci. U. S. A.* 106, 9099–9104.
- (8) Deering-Rice, C. E., Shapiro, D., Romero, E. G., Stockmann, C., Bevans, T. S., Phan, Q. M., Stone, B. L., Fassl, B., Nkoy, F., Uchida, D. A., Ward, R. M., Veranth, J. M., and Reilly, C. A. (2015) Activation of Transient Receptor Potential Ankyrin-1 (TRPA1) by Insoluble Particulate Material and Association with Asthma. *Am. J. Respir. Cell Mol. Biol.* 53, 893–901.
- (9) Deering-Rice, C. E., Stockmann, C., Romero, E. G., Lu, Z., Shapiro, D., Stone, B. L., Fassl, B., Nkoy, F., Uchida, D. A., Ward, R. M., Veranth, J. M., and Reilly, C. A. (2016) Characterization of transient receptor potential vanilloid-1 (TRPV1) variant activation by coal fly ash particles and associations with altered TRPA1 expression and asthma. *J. Biol. Chem.* 291, 24866.
- (10) Mio, T., Romberger, D. J., Thompson, A. B., Robbins, R. A., Heires, A., and Rennard, S. I. (1997) Cigarette smoke induces interleukin-8 release from human bronchial epithelial cells. *Am. J. Respir. Crit. Care Med.* 155, 1770–1776.

- (11) Simon, S. A., and Liedtke, W. (2008) How irritating: the role of TRPA1 in sensing cigarette smoke and aerogenic oxidants in the airways. *J. Clin. Invest.* 118, 2383–2386.
- (12) Bessac, B. F., Sivula, M., von Hehn, C. A., Escalera, J., Cohn, L., and Jordt, S.-E. (2008) TRPA1 is a major oxidant sensor in murine airway sensory neurons. *J. Clin. Invest.* 118, 1899–1910.
- (13) Deering-Rice, C. E., Romero, E. G., Shapiro, D., Hughen, R. W., Light, A. R., Yost, G. S., Veranth, J. M., and Reilly, C. A. (2011) Electrophilic Components of Diesel Exhaust Particles (DEP) Activate Transient Receptor Potential Ankyrin-1 (TRPA1): A Probable Mechanism of Acute Pulmonary Toxicity for DEP. *Chem. Res. Toxicol.* 24, 950–959.
- (14) Baraldi, P. G., Preti, D., Materazzi, S., and Geppetti, P. (2010) Transient Receptor Potential Ankyrin 1 (TRPA1) Channel as Emerging Target for Novel Analgesics and Anti-Inflammatory Agents. *J. Med. Chem.* 53, 5085–5107.
- (15) Nassini, R., Pedretti, P., Moretto, N., Fusi, C., Carnini, C., Facchinetti, F., Viscomi, A. R., Pisano, A. R., Stokesberry, S., Brunmark, C., Svitacheva, N., McGarvey, L., Patacchini, R., Damholt, A. B., Geppetti, P., and Materazzi, S. (2012) Transient receptor potential ankyrin 1 channel localized to non-neuronal airway cells promotes non-neurogenic inflammation. *PLoS One* 7, e42454.
- (16) Mukhopadhyay, I., Gomes, P., Aranake, S., Shetty, M., Karnik, P., Damle, M., Kuruganti, S., Thorat, S., and Khairatkar-Joshi, N. (2011) Expression of functional TRPA1 receptor on human lung fibroblast and epithelial cells. *J. Recept. Signal Transduction Res.* 31, 350–358.
- (17) Deering-Rice, C. E., Johansen, M. E., Roberts, J. K., Thomas, K. C., Romero, E. G., Lee, J., Yost, G. S., Veranth, J. M., and Reilly, C. A. (2012) Transient receptor potential vanilloid-1 (TRPV1) is a mediator of lung toxicity for coal fly ash particulate material. *Mol. Pharmacol.* 81, 411–419.
- (18) Nassenstein, C., Kwong, K., Taylor-Clark, T., Kollarik, M., Macglashan, D. M., Braun, A., and Undem, B. J. (2008) Expression and function of the ion channel TRPA1 in vagal afferent nerves innervating mouse lungs. *J. Physiol.* 586, 1595–1604.
- (19) Shapiro, D., Deering-Rice, C. E., Romero, E. G., Hughen, R. W., Light, A. R., Veranth, J. M., and Reilly, C. A. (2013) Activation of Transient Receptor Potential Ankyrin-1 (TRPA1) in Lung Cells by Wood Smoke Particulate Material. *Chem. Res. Toxicol.* 26, 750–758.
- (20) Sun, W., Wang, Z., Cao, J., Wang, X., Han, Y., and Ma, Z. (2014) Enhanced production of nitric oxide in A549 cells through activation of TRPA1 ion channel by cold stress. *Nitric Oxide* 40, 31–35.
- (21) Buch, T. R., Schafer, E. A., Demmel, M. T., Boekhoff, I., Thiermann, H., Gudermann, T., Steinritz, D., and Schmidt, A. (2013) Functional expression of the transient receptor potential channel TRPA1, a sensor for toxic lung inhalants, in pulmonary epithelial cells. *Chem.-Biol. Interact.* 206, 462–471.
- (22) Singh, P., DeMarini, D. M., Dick, C. A., Tabor, D. G., Ryan, J. V., Linak, W. P., Kobayashi, T., and Gilmour, M. I. (2004) Sample characterization of automobile and forklift diesel exhaust particles and comparative pulmonary toxicity in mice. *Environ. Health Perspect.* 112, 820–825.
- (23) Deering-Rice, C. E., Nguyen, N., Lu, Z., Cox, J. E., Shapiro, D., Romero, E. G., Mitchell, V. K., Burrell, K. L., Veranth, J. M., and Reilly, C. A. (2018) Activation of TRPV3 by Wood Smoke Particles and Roles in Pneumotoxicity. *Chem. Res. Toxicol.* 31, 291–301.
- (24) Hazari, M. S., Haykal-Coates, N., Winsett, D. W., Krantz, Q. T., King, C., Costa, D. L., and Farraj, A. K. (2011) TRPA1 and Sympathetic Activation Contribute to Increased Risk of Triggered Cardiac Arrhythmias in Hypertensive Rats Exposed to Diesel Exhaust. *Environ. Health Perspect.* 119, 951–957.
- (25) Bessac, B. F., and Jordt, S. E. (2008) Breathtaking TRP channels: TRPA1 and TRPV1 in airway chemosensation and reflex control. *Physiology* 23, 360–370.
- (26) Bessac, B. F., Sivula, M., von Hehn, C. A., Escalera, J., Cohn, L., and Jordt, S. E. (2008) TRPA1 is a major oxidant sensor in murine airway sensory neurons. *J. Clin. Invest.* 118, 1899–1910.
- (27) Taylor-Clark, T. E., McAlexander, M. A., Nassenstein, C., Sheardown, S. A., Wilson, S., Thornton, J., Carr, M. J., and Undem, B. J. (2008) Relative contributions of TRPA1 and TRPV1 channels in the activation of vagal bronchopulmonary C-fibres by the endogenous autacoid 4-oxononanal. *J. Physiol.* 586, 3447–3459.
- (28) Jaramillo, I. C., Sturrock, A., Ghiassi, H., Woller, D. J., Deering-Rice, C. E., Lighty, J. S., Paine, R., Reilly, C., and Kelly, K. E. (2018) Effects of Fuel Components and Combustion Particle Physicochemical Properties on Toxicological Responses of Lung Cells. *J. Environ. Sci. Health, Part A: Toxic/Hazard. Subst. Environ. Eng.* 53, 295–309.
- (29) Singh, A., Misra, V., Thimmulappa, R. K., Lee, H., Ames, S., Hoque, M. O., Herman, J. G., Baylin, S. B., Sidransky, D., Gabrielson, E., Brock, M. V., and Biswal, S. (2006) Dysfunctional KEAP1-NRF2 interaction in non-small-cell lung cancer. *PLoS Med.* 3, e420.
- (30) Poerschke, R. L., and Moos, P. J. (2011) Thioredoxin reductase 1 knockdown enhances selenazolidine cytotoxicity in human lung cancer cells via mitochondrial dysfunction. *Biochem. Pharmacol.* 81, 211–221.